Proceedings Paper:

Agnew, G, Grier, A, Taimre, T et al. (12 more authors) (2015) Terahertz quantum cascade laser bandwidth prediction. In: Microwave Photonics (MWP), 2015 International Topical Meeting on. 2015 IEEE International Topical Meeting on Microwave Photonics (MWP), 26-29 Oct 2015, Paphos, Cyprus. IEEE .

https://doi.org/10.1109/MWP.2015.7356671

Terahertz quantum cascade laser bandwidth prediction

Gary Agnew, *Member, IEEE,* Andrew Grier, Thomas Taimre, *Associate Member, IEEE,* Yah Leng Lim, Zoran Ikonić, Paul Dean, Suraj P. Khanna, Mohammad Lachab, Alexander Valavanis, Jonathan Cooper, Paul Harrison, Edmund H. Linfield, A. Giles Davies, Dragan Indjin, and Aleksandar D. Rakić, *Senior Member, IEEE*

***Abstract*—Recent research shows that terahertz quantum cascade lasers are well-suited to high speed free space communication. The results of both theoretical and laboratory work indicate the devices are able to deliver bandwidths in the gigahertz to tens of gigahertz range without the burden of relaxation oscillations found in diode lasers. Using a novel rate equation model we explore the frequency response characteristics of a real device and report on the finding of a strongly peaked bias current-dependent response.**

***Index Terms*—Free space communication, terahertz quantum cascade laser, bandwidth**

I. Introduction

Reduced rate equation (RRE) models are a computationally efficient means of exploring laser dynamics and have been used widely to do so [1], [2], [3]. Bandwidth estimation for quantum cascade lasers (QCLs) has traditionally been carried out through laboratory measurement [4], and theoretically, by means of small signal models developed from the RREs [3], [5]. The RRE parameters (gain, carrier lifetimes, and injection efficiencies) used in such models are usually constant, and are specific to the lattice temperature and electric field (bias) for which they were developed. This restricts their use somewhat, as both the static and dynamic behavior of the laser is strongly affected by the RRE parameters. They must therefore be re-determined if temperature or bias change significantly.

We have taken a different approach by developing a RRE model with parameters that are functions of both temperature and bias. We create these functions by calculating all parameters using full-multi subband QCL energy-balance scattering rate transport Schrödinger–Poisson (S–P) solver [6] for a range of temperatures and biases, and then interpolate the calculated values to find values at a specified temperature and bias whilst solving the RREs. This gives our model the ability to produce a realistic output, whatever the lattice temperature and bias. Under large signal conditions the temperature (due to self-heating) and bias are ever-changing, and we manage this by continuously updating the parameters as the solution of the RREs progresses. This necessitates the use of a thermal model in conjunction with the RREs, as the (unknown) lattice temperature has to be determined from the cold finger temperature, self-heating power, and the characteristics of the thermal circuit.

Using our RRE together with an ODE solver, we can easily assess the bandwidth of a QCL for any cold finger temperature and drive current waveform. We do this by superimposing a small test sinusoid on the DC bias current and observing the corresponding response (optical output power).

In this paper we present the frequency response and bandwidth predicted by our model at a fixed cold finger temperature, for a range of bias currents. We also present the time-resolved pulse response at the maximum-bandwidth-bias on a laser dynamics timescale and observe an absence of relaxation oscillations.

II. Exemplar device model

The exemplar QCL we chose to model is a GaAs/AlGaAs Fabry–Pérot, single-mode, 90 period, bound-to-continuum terahertz (THz) QCL emitting at 2.59 THz. More information about the structure of the device can be found in [7], and the full set of rate and thermal equations for our model is detailed in [8]. The rate equation parameters comprising gain, carrier lifetimes, and injection efficiencies, were calculated specifically for our exemplar QCL using the structure of the device as input to a S–P solver for the full rate equations. We validated the steady state behavior of our model by simulating light-current (L–I) curves and comparing them with laboratory measurements under the same conditions (see Fig. 1).

III. Results and discussion

Our frequency response simulation was done at a cold finger temperature of 15 Kelvin, for four bias currents — 425 mA, 440 mA, 450 mA, and 460 mA. In each case a test sinusoid of 20 μA peak-to-peak amplitude was superimposed on the bias current for a range of frequencies from 200 MHz to 30 GHz. The result, shown in Fig. 2, demonstrates the 3 dB bandwidth rising to a maximum just before the peak of the L–I curve at 460 mA. To the right of the L–I curve's peak the bandwidth

G. Agnew, Y. L. Lim, and A. D. Rakić are with the School of Information Technology and Electrical Engineering, The University of Queensland, Brisbane, Queensland, 4072, Australia (corresponding author can be reached at phone: +61-7-3365-8305; fax: +61-7-3365-4999; e-mail: g.agnew@uq.edu.au).

T. Taimre is with the School of Mathematics and Physics, The University of Queensland, Brisbane, Queensland, 4072, Australia

A. Grier, D. Indjin, Z. Ikonić, P. Dean, S. Khanna, M. Lachab, A. Valavanis, J. Cooper, E. Linfield, and A. Davies are with the School of Electronic and Electrical Engineering, University of Leeds, Leeds LS2 9JT, U.K.

P. Harrison is with the Materials and Engineering Research Institute, Sheffield Hallam University, Sheffield, S1 1WB, United Kingdom

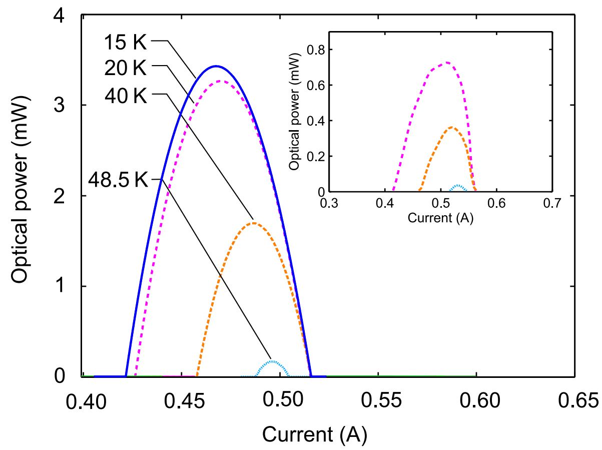

Fig. 1. (Color online) RRE simulated L–I curves for four cold finger temperatures. Inset: measured L–I characteristics at some of the same temperatures.

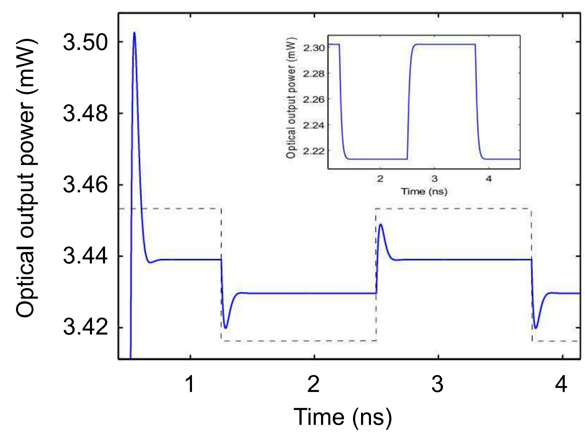

Fig. 3. RRE simulated time-resolved pulse response. The test pulse train is a square wave of amplitude 1 mA and period 2.5 ns superimposed on a bias current of 460 mA (timing shown as dashed lines in main figure). Inset: pulse response for the same small signal stimulus at a bias current of 425 mA.

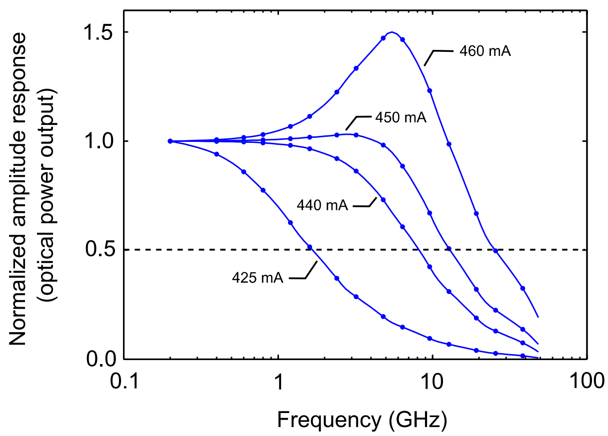

Fig. 2. RRE simulated frequency response, at a cold finger temperature of 15 K, for four bias currents. The curves are normalized for comparison, and rapidly diminish with bias current when plotted on an absolute scale.

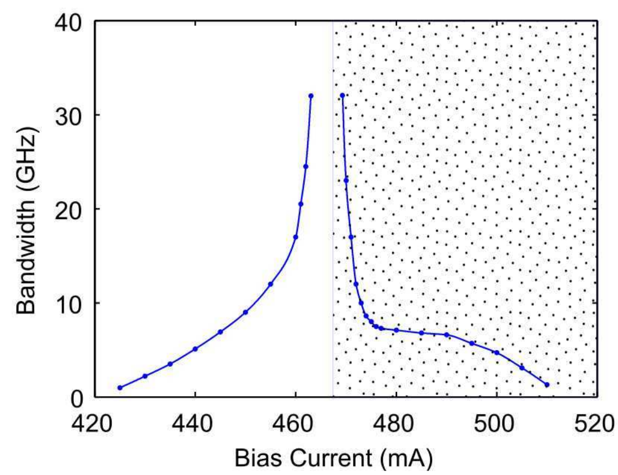

Fig. 4. Bandwidth against bias current. Each data point was obtained by finding the 3 dB cutoff in the frequency response (0.5 in Fig. 2). The left hand curve represents the bandwidth for the ascending part of the L–I curve (Fig. 1) and the right hand one the descending part.

falls with increasing current, but not in a symmetrical manner (not shown in the figure).

The curves in Fig. 2 are normalized for comparison. On an absolute scale the output power of the time–varying component is greatest at low bias currents, where the slope efficiency is best. At higher bias currents the optical output power produced by the test signal diminishes due to falling slope efficiency and vanishes at the crest of the L–I curve, making it impossible to obtain a meaningful frequency response at that point. Our test signal was small enough to reach within 1 mA of the crest without being adversely affected by nonlinear effects.

A salient feature of Fig. 2 is the increasingly peaked frequency response as the crest of the L–I curve is approached. Despite this, the time-resolved pulse response for the same current, 460 mA, shows no trace of oscillatory response (see Fig. 3), corroborating the findings of others [9], [10]. The test signal for the time trace was a square wave of amplitude 1 mA peak-to-peak and 2.5 ns period (corresponding frequency 400 MHz). For comparison, the pulse response at 425 mA, shown in the inset, appears as a damped response.

Dependence of the modulation bandwidth on bias current (inferred from the frequency response curves) is shown in Fig. 4. The left hand section of graph corresponds to the family of curves in Fig. 2. The right hand (shaded) section corresponds to bias currents on the right hand (descending) part of the L–I curve, and would not normally be used due to the higher heat dissipated at higher bias currents.

Although the graph appears to have a singularity at the crest of the L–I curve, the bandwidth of the device will in fact be limited to under 30 GHz. We note the asymmetry of the bandwidth vs. bias current characteristic, and in particular the bandwidth plateau at about 480 mA that does not exist for the left-hand half of the L–I curve. The large apparent gain in bandwidth at and above 460 mA seen in Fig. 4 is offset by an optical output power that diminishes at least as fast as the bandwidth increases.

IV. Conclusion

Using a novel RRE model of a real bound-to-continuum 2.59 THz QCL, we have found the frequency response and hence bandwidth of the device for a variety of bias conditions. Our results show that bandwidth increases with bias current, is highest at the crest of the L–I curve, and then falls off again in an asymmetrical manner with further increases in bias current. We observe that despite a sharply peaked frequency response at the crest of the L–I characteristic, the time-resolved pulse response shows no relaxation oscillation.

Acknowledgments

This research was supported under Australian Research Councils Discovery Projects funding scheme (DP 120 103703). We also acknowledge support of the ERC 'NOTES' and 'TOSCA' programmes, the EPSRC (UK), the Royal Society, the Wolfson Foundation, and the European Cooperation in Science and Technology (COST) Action BM1205. Y.L.L. acknowledges support under the Queensland Governments Smart Futures Fellowships programme.

References

[1] A. Hamadou, J. L. Thobel, and S. Lamari, "Modelling of temperature effects on the characteristics of mid-infrared quantum cascade lasers," *Opt. Commun.*, vol. 281, no. 21, pp. 5385–5388, 2008.

[2] A. Hamadou, S. Lamari, and J. L. Thobel, "Dynamic modeling of a midinfrared quantum cascade laser," *J. Appl. Phys.*, vol. 105, no. 9, pp. 093 116–0 931 166, 2009.

[3] Y. Petitjean, F. Destic, J. C. Mollier, and C. Sirtori, "Dynamic modeling of terahertz quantum cascade lasers," *IEEE J. Sel. Top. Quant. Electron.*, vol. 17, no. 1, pp. 22–29, 2011.

[4] R. Martini, C. Gmachl, R. Paiella, F. Capasso, C. Glazowski, R. Murawski, E. A. Whittaker, C. G. Bethea, H. Y. Hwang, D. L. Sivco, J. N. Baillargeon, A. Y. Cho, and H. C. Liu, "Analog and digital high-speed modulation of quantum-cascade laser," in *Proc. SPIE-Int. Soc. Opt. Eng.*, vol. 4995, 2003, pp. 169–175.

[5] J. Faist, *Quantum Cascade Lasers*. Oxford University Press, 2013.

[6] V. D. Jovanović, S. Höfling, D. Indjin, N. Vukmirović, Z. Ikonić, P. Harrison, J. P. Reithmaier, and A. Forchel, "Influence of doping density on electron dynamics in GaAs/AlGaAs quantum cascade lasers," *J. Appl. Phys.*, vol. 99, no. 10, pp. 103 106–1 031 069, 2006.

[7] A. D. Rakić, T. Taimre, K. Bertling, Y. L. Lim, P. Dean, D. Indjin, Z. Ikonić, P. Harrison, A. Valavanis, S. P. Khanna, M. Lachab, S. J. Wilson, E. H. Linfield, and A. G. Davies, "Swept-frequency feedback interferometry using terahertz frequency QCLs: A method for imaging and materials analysis," *Opt. Express*, vol. 21, no. 19, pp. 22 194–22 205, 2013.

[8] G. Agnew, A. Grier, T. Taimre, Y. Lim, M. Nikolić, A. Valavanis, J. Cooper, P. Dean, S. Khanna, M. Lachab, E. Linfield, A. Davies, P. Harrison, Z. Ikonić, D. Indjin, and A. Rakić, "Efficient prediction of terahertz quantum cascade laser dynamics from steady-state simulations," *Appl. Phys. Lett.*, vol. 106, no. 16, pp. 161 105–1–4, 2015.

[9] R. Martini, R. Paiella, F. Capasso, C. Gmachl, H. Y. Hwang, D. L. Sivco, A. Y. Cho, E. A. Whittaker, and H. C. Liu, "Absence of relaxation oscillation in quantum cascade lasers verified by high-frequency modulation," in *CLEO Europe - Technical Digest*, 2001, pp. xxxiii–xxxiv.

[10] R. Paiella, R. Martini, F. Capasso, C. Gmachl, H. Y. Hwang, D. L. Sivco, J. N. Baillargeon, A. Y. Cho, E. A. Whittaker, and H. C. Liu, "High-frequency modulation without the relaxation oscillation resonance in quantum cascade lasers," *Appl. Phys. Lett.*, vol. 79, no. 16, pp. 2526–2528, 2001.